

Densification and properties of in-situ synthesized ZrB₂-SiC composites from ZrO₂, B₄C and SiC system

Kübra Gürcan, Burcu Yılmaz and Erhan Ayas*

Faculty of Engineering, Department of Materials Science & Engineering, İki Eylül Campus, Anadolu University, TR-26480 Eskişehir, Türkiye

Zirconium diboride-silicon carbide (ZrB₂-SiC) ceramics were in-situ synthesized and densified by the spark plasma sintering (SPS) method using ZrO₂, B₄C and SiC as starting powders. Both synthesis and densification processes were successfully accomplished in a single SPS cycle with one step heating schedules which were designed by considering thermodynamic calculations made by Factsage software. One step synthesis/densification schedule at 1950 °C with a 30 min hold time under 50 MPa uniaxial pressure lead to obtain ZrB₂-SiC ceramics up to 93% of its theoretical density. Considering the literature, low hardness values (max. 17.55 GPa) were achieved which were directly attributed to the low bonding between ZrB₂ and SiC grains in terms of the residual stresses occurred during the synthesis and cooling steps. Fracture toughness of the ceramics was 4.12 MPa.m^{1/2} and crack deflection and microcracking were believed to be primary toughening mechanisms of ZrB₂-SiC composites.

Key words: UHTC, ZrB₂-SiC, in-situ synthesis, SPS.

Introduction

Among the class of ultra-high temperature ceramics (UHTC), ZrB₂ is of particular interest due to its extremely high melting temperature (3245 °C) high modulus (≈500 GPa), high hardness (21-28 GPa), high thermal conductivity, low volatility, good thermo-mechanical properties and excellent corrosion resistance. These unique combinations of properties make ZrB₂ a promising candidate for extreme applications such as thermal protection components like leading edges in hypersonic atmospheric reentry vehicles, rocket nozzles, and scramjet components, where operating temperatures can exceed 3000 °C [1-4]. On the other hand, densification of monolithic ZrB₂ is a very difficult process in terms of its extreme refractory character. The consolidation of boride materials were generally achieved through conventional sintering methods like hot pressing, pressureless sintering, and reactive densification processes (ex. Reactive HP) using additives like SiC, MoSi₂, TaSi₂, Si₃N₄ or metallic additives, resulting in materials with large grain sizes and consequently poor mechanical properties [5-10].

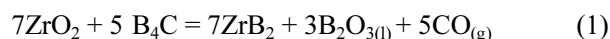
As it is well known, spark plasma sintering (SPS) is one of the favorable methods to densify such highly covalent bonded materials. This technique, reduces the sintering temperature, shortens the sintering time and improves the mechanical and thermal properties as a

result of joule and direct heating generated by high pulsed electric current [11]. SPS is also utilized for both synthesis and sintering in one single processing step, like other reactive densification methods such as reactive spark plasma sintering (R-SPS) starting from appropriate reactants. Alternatively, to the classical approach based on the fabrication of commercial powders, few studies have been carried out on the R-SPS sintering of some borides [12-16].

In the current study, in-situ synthesis of ZrB₂-SiC based ceramics from starting powders of zirconium oxide (ZrO₂), boron carbide (B₄C) and silicon carbide (SiC) with the SPS technique were studied. Effect of SPS parameters such as temperature and h-BN coating of dies combined with thermodynamic considerations were investigated.

Materials and Methods

Commercially available monolithic ZrO₂ (Tosoh-TZ0, average particle size: 40-100 nm), B₄C (Alfa Aesar, average particle size: < 10 μm) and SiC (H.C. Starck-Grade UF-10, average particle size: 0.7 μm) powders were used as starting powders. The powder mixtures of ZrO₂ and B₄C with the mol ratio of 7:5 according to reaction (1) and 25 vol % SiC were used.



Powders were planetary ball milled (Pulverisette, P6, Fritsch) for 90 min in 2-propanol at a rotational speed of 450 rpm by using Si₃N₄ grinding media. The slurry

*Corresponding author:
Tel : +90(222)-322 36 62-6306
Fax: +90(222)-323 95 01
E-mail: erayas@anadolu.edu.tr

was then dried in a rotary evaporator and the powders were sieved under $250\ \mu\text{m}$ in order to break up agglomerates.

In-situ synthesis of ZrB_2 -SiC composites was carried out under vacuum atmosphere in a SPS furnace (HPD-50, FCT GmbH, Germany). The powders were put into a graphite die 20 mm in diameter isolated with a graphite foil to prevent the reaction between powders and die. The temperature was increased with a controlled electric pulsed current and measured on the graphite die surface with an optical pyrometer. The heating rate was kept constant as $50\ ^\circ\text{C}/\text{min}$ during all process. The compacts were sintered at $1850\ ^\circ\text{C}$ and $1950\ ^\circ\text{C}$ with a 30 min holding time. The pressure was increased from 15 MPa to 50 MPa during the whole sintering process. To understand the effect of h-BN coating on the microstructural evaluation, graphite foil was coated with and without h-BN.

The bulk densities were determined by using the Archimedes method after removing the surface layer from the SPS samples by grinding. For XRD analysis sintered samples were crushed and ground under $63\ \mu\text{m}$. Quantitative phase analysis was accomplished by using an X-ray diffractometer (Rigaku Rint2200 series) at a scan speed of $1^\circ/\text{min}$. The polished and fractured surfaces of the samples were examined using a scanning electron microscope (Supra 50 VP, Zeiss-Germany) equipped with an EDX detector (Oxford Instruments, UK). The Vickers hardness (Hv_{10}) from the polished surfaces of the sintered samples was measured using an indenter (EMCOTest, MIC-Germany) with a load of 10 kg. The fracture toughness (K_{IC}) of the samples was evaluated from radial cracks formed during the indentation test [17].

Result and Discussions

Effect of sintering temperature on microstructural development

Applied SPS conditions and calculated relative densities of the samples after sintering were given in Table 1. Comparing the relative density values, higher sintering temperature was required to densification of ZrB_2 -SiC ceramics. The displacement curves of ZS1 and ZS2 achieved during the SPS process were given in Fig. 1.

In both figures, the first consolidation of powders starts at $850\ ^\circ\text{C}$ and a rapid increase in the displacement is observed up to $1150\ ^\circ\text{C}$. The Gibb's free energy of reaction (1) as a function of temperature and partial pressure of formed gases in the standard state and SPS conditions ($\approx 10^{-2}$ mbar) was given in Fig. 2.

It should be noted that the partial pressure of formed gases affects the reaction temperature. The onset temperature of the reaction is approximately $1210\ ^\circ\text{C}$ ($\Delta G_{1210\ ^\circ\text{C}} = -6470.1\ \text{J}$) in the standard state when the partial pressure was 10^{-2} mbar, it decreased to $850\ ^\circ\text{C}$

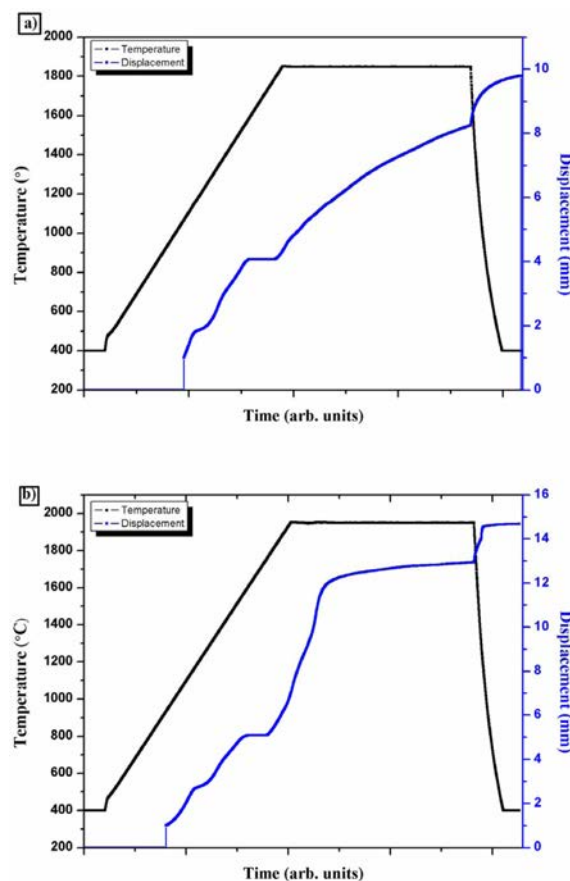


Fig. 1. The displacement curves of (a) ZS1 (b) ZS2.

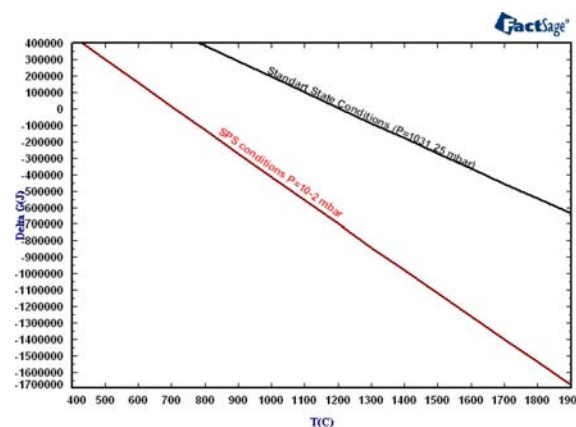


Fig. 2. The Gibb's free energy change of reaction (1) as a function of temperature and partial pressure.

($\Delta G_{850\ ^\circ\text{C}} = -205049.1\ \text{J}$). It is implied that reaction (1) becomes favorable at $\approx 1210\ ^\circ\text{C}$. However, the partial pressures of gaseous product in vacuum (10^{-2} mbar) decreases the reaction temperature, so the reaction (1) starts at $\approx 850\ ^\circ\text{C}$. This indicates that observed rapid displacement change between $850\ ^\circ\text{C}$ and $1150\ ^\circ\text{C}$ was a result of the formation of reaction products. Another remarkable point was the observed second rapid displacement between $1150\ ^\circ\text{C}$ and $1600\ ^\circ\text{C}$. According to thermodynamic considerations a relatively high

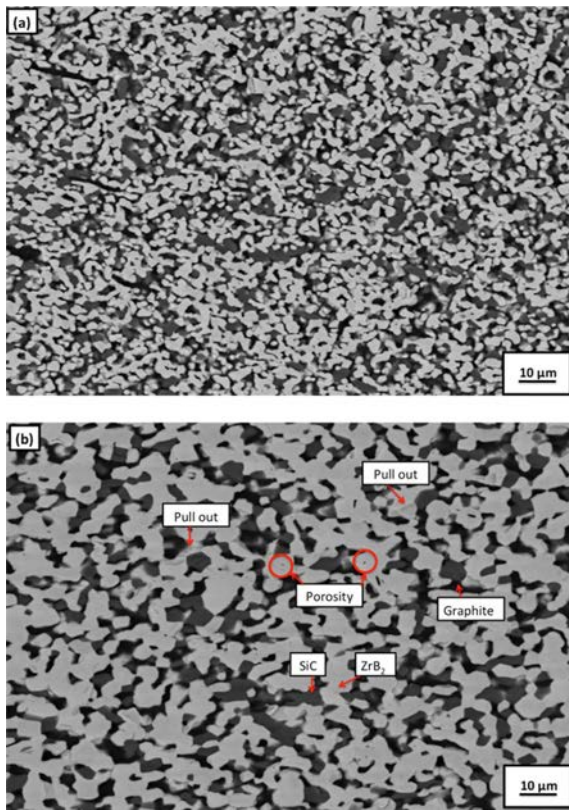


Fig. 3. Back-scattered SEM images taken from polished surface of (a) ZS1 and (b) ZS2.

amount of liquid and gaseous phases composed of B_2O_3 and CO formed above $1150\text{ }^\circ\text{C}$. A considerable amount of these types of phases confirmed to be squeezed out from the graphite die during the SPS process. However, in terms of the die setup a little amount of these phases were believed to be in motion during the process which is thought to be the main reason for the rapid displacement between $1150\text{ }^\circ\text{C}$ and $1600\text{ }^\circ\text{C}$. The densification of composites appeared to be start at $1800\text{ }^\circ\text{C}$. However, the displacement of the punches did not stop during the whole holding duration when sintering was carried out at $1850\text{ }^\circ\text{C}$. In contrast, the displacement of the punches decreased within half of holding time and ended after 25 minutes at $1950\text{ }^\circ\text{C}$. This indicates that consolidation of ZrB_2 -SiC composites was achieved at higher sintering temperature.

Back-scattered SEM images taken from polished surface of ZS1 and ZS2 were given in Fig. 3. In both figures white contrasted areas represents ZrB_2 , grey contrasted areas represent SiC and dark contrasted areas represents C phases as confirmed with EDX. C was formed due to the proximity of the sintered material to the graphite die and plungers. Formation of ZrB_2 -SiC material was not exactly completed at the $1850\text{ }^\circ\text{C}$. According to the theoretical density of ZrB_2 -25%vol SiC composites (5.38 g/cm^3), the measured relative density of ZS2 is 89%, which is the highest value of samples. However, C containing phases were

also observed on microstructure. In order to calculate more accurate results, theoretical density of ZS2 samples was determined from the SEM images by using Scandium image analysis software with using the amount of phase composition of the sample. According to the image analysis results, relative density of ZS2 sample is 93%, which is the highest value of the all samples. Aside from C-containing, pull out defects and residual porosity were observed in both microstructures. On the other hand an excessive grain growth for both ZrB_2 and SiC phases were observed due to the increase in sintering temperature.

Effect of h-BN coating of graphite foil on microstructural development

It was found that, effect of the h-BN coating of graphite foil had very significant role on the formation of materials in our previous study [18]. In order to investigate h-BN coating on formation of ZrB_2 -SiC composites, ZS1 and ZS2 samples were carried out with h-BN coated graphite foil and labelled ZS1-c and ZS2-c, respectively. Back-scattered SEM images taken from the polished surfaces of ZS1-c and ZS2-c were

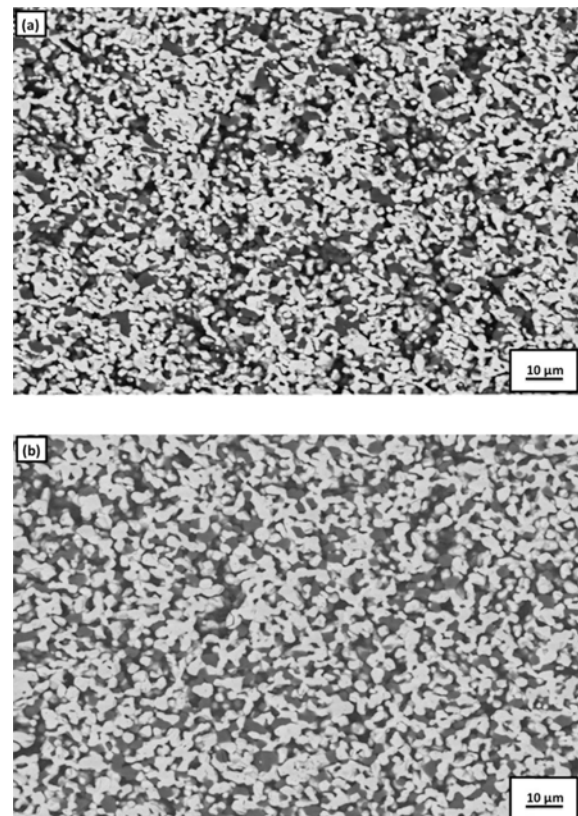


Fig. 4. Back-scattered SEM images taken from polished surface of (a) ZS1-c and (b) ZS2-c.

illustrated in Fig. 4.

Considering the SEM images, h-BN coating was found to have a negative effect on the densification of

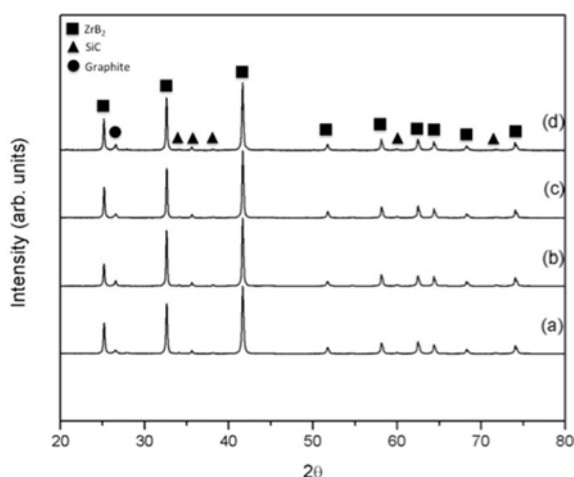


Fig. 5. Comparative XRD patterns of the samples (a) ZS1, (b) ZS2, (c) ZS1-c, (d) ZS1-d.

composites. C containing phases, glassy phases, pull out defects and residual porosities were obvious in both samples. As it is known, h-BN is traditionally used as parts of high temperature equipment's because of its excellent properties such as high thermal and chemical stability, high thermal conductivity [19]. Direct heating of graphite mold by the pulse current provides rapid heat generation in extremely short duration in SPS process. It is believed that generated heat is transferred much more quickly, so formation rate of reaction increases in the h-BN coated samples due to its high thermal conductivity. However, calculated relative density values of ZS1-c and ZS2-c were the lower than that of the ZS2 which shows the highest relative density of 95%. It is considered that liquid and/or gaseous reaction products could not squeezed out when h-BN is coated of the graphite foil which lead to an entrapment of these mentioned phases in the grain boundaries during the cooling.

Comparative XRD patterns of the ZS1, ZS2, ZS1-c and ZS2-c were given Fig. 5. ZrB₂ and SiC were detected as the major crystalline phases, confirming the formation of a desired composition. Besides, the diffraction peak of graphite was detected which was also confirmed with SEM images.

Mechanical properties

Hardness and fracture toughness of the samples were determined by Vickers indentation tests (Hv10). Measured hardness and the indentation fracture toughness of the samples were presented in Table 2. The ZS2 sample had the highest hardness value (17.55 GPa). Low hardness values of ZS1, ZS1-c and ZS2-c can be attributed to the low relative density and microstructural features. Another reason that might be contributed to the lower hardness values is the SPS conditions. As mentioned before, applied uniaxial pressure, high temperature, high heating and cooling rates during the

Table 1. Experimental conditions and relative densities of the SPS'ed samples.

Sample Name	hBN coating	Sintering temperature (°C)	Relative Density (%)
ZS1	-	1850	87
ZS2	-	1950	93
ZS1-c	+	1850	79
ZS2-c	+	1950	78

Table 2. Measured hardness and the indentation fracture toughness of the samples.

Sample	Hardness (Hv20-GPa)	Fracture toughness (MPa.m ^{1/2})
ZS1	9.28 ± 0.32	-
ZS2	17.55 ± 0.05	4.12 ± 0.17
ZS1-c	4.53 ± 0.17	-
ZS2-c	4.94 ± 0.07	-

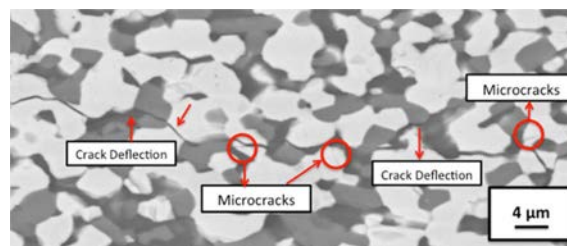


Fig. 6. Representative SEM images of the crack paths originating during Vickers indentation achieved from the sample ZS2.

formation process are thought to cause internal stresses. It is found that thermal mismatch on the anisotropic materials (HfB₂, ZrB₂, B₄C, Al₂O₃, etc.) would lead to the formation of microstructural defects like pull outs, micro cracks, causing a reduction of hardness.

The fracture toughness of the ZS1, ZS1-c and ZS2 cannot be measured because of the infinitely longest crack propagation. ZS2 has a toughness value of 4.12 MPa.m^{1/2}. The obtained value is similar with previously found values for ZrB₂-SiC composites, which range from 4-6 MPa.m^{1/2} [20]. Comparative crack paths induced during the Vickers indentation of the sample ZS2 were given in Fig. 6. It is found that crack deflection and opening of ZrB₂/SiC interfaces and some microcracking of ZrB₂ grains were observed. As it well known, high residual stresses cause microcracks, which emerge at the interfaces as a consequence of the mismatch of the thermal expansion coefficient between ZrB₂ and SiC. The occurrence of crack deflection and microcracks could have increased the fracture toughness.

Conclusions

In situ synthesis and sintering of ZrB₂-SiC ceramics were achieved by spark plasma sintering method.

Different from the relevant literature, ZrO₂, B₄C and SiC were used for starting powders. During the experiments, sintering was carried out 1850 and 1950 °C with 30 min holding and the pressure was increased from 15 MPa to 50 MPa during the whole sintering process. Besides sintering temperature, effect of h-BN coating of graphite foil was successfully investigated. h-BN coating was found to have a negative effect microstructural stability because of the entrapment of liquid and/or gaseous phases which were not squeezed out in the grain boundaries during the cooling. Higher density and better microstructural stability were obtained in ZS2 sample which was sintered without h-BN coating at 1950 °C. Considering mechanical properties, hardness value was low because of the low bonding between ZrB₂ and SiC grains in terms of the residual stresses occurred during the synthesis and cooling steps. Crack deflection and micro cracking were the main mechanisms for increasing the fracture toughness.

Acknowledgments

This work was supported by Anadolu University Scientific Research Project [grant number 1501F020].

References

1. K. Upadhyaya, J.M. Yang, and W.P. Hoffman, *J. Am. Ceram. Soc. Bull.* 76[12] (1997) 51-56.
2. E. Wuchina, M. Opeka, S. Causey, K. Buesking, J. Spain, A. Cull, J. Routbort, and F. Guitierrez-Mora, *J. Mater. Sci.* 39[19] (2004) 5939-5949.
3. D.M. Van-Wie, D.G.J. Drewry, D.E. King, and C.M. Hudson, *J. Mater. Sci.* 39[19] (2004) 5915-5924.
4. W.G. Fahrenholtz, G.E. Hilmas, I.G. Talmy, and J.A. Zaykoski, *J. Am. Ceram. Soc.* 90 [5] (2007) 1347-1364.
5. E.V. Clougherty, P.L. Poher, and L.Kaufman, *Trans. Met. Soc. AIME*, 242 (1968) 1077-1082.
6. J.R. Fenter, *SAMPE Quarterly* 2 (1971) 1-15.
7. W.M. Guo, Z.G. Yang, and G.J. Zhang, *Mater. Lett.* 83 (2012) 52-55.
8. D.W. Ni, G.L. Zhang, Y.M. Kan, P.L. Wang, *Int. J. Appl. Ceram. Technol.* 7[6] (2010) 830-836.
9. G.J. Zhang, W.M.Guo, D.W. Ni, and Y.M. Kan, *The 16th Int. Sym. on Boron, Borides and Related Materials, Journal of Physics: Conference Series*.176 (2009) 012041.
10. L. Silvestroni, and D. Sciti, *J. Am. Ceram. Soc.* 94[6] (2011) 1920-1930.
11. D.V. Quach, and J.R. Groza, Woodhead Publishing. 10 (2010) 249-247.
12. C.F. Hu, Y. Sakka, T. Uchikoshi, T. Suzuki, B.K. Jang, S. Grasso, and G. Suarez, *Key Eng. Mater.* 165[8] (2010) 434-435.
13. U.A. Tamburini, Y. Kodera, M. Gasch, C. Unuvar, Z.A. Munir, M. Ohyanagi, and S.M. Johnson, *J. Mater. Sci.* 41 (2006) 3097-3104.
14. H. Yuan, J. Li, Q. Shen, and L. Zhang, *Int. J. Refract. Met. Hard. Mater.* 34 (2012) 3-7.
15. H. Yuan, J. Li, Q. Shen, and L. Zhang, *Int. J. Refract. Met. Hard. Mater.* 36 (2013) 225-231.
16. H. Wang, S.H. Lee, and H.D. Kim, *J. Am. Ceram. Soc.* 95[5] (2012) 1493-1496.
17. A.G. Evans, and E.A. Charles, *J. Am. Ceram.* 59 (1976) 371-372.
18. K. Gürcan, and E. Ayas, *Ceram. Inter.* 43 (2017) 3547-3555.
19. A. Lipp, K.A. Schwetz, and K. Hunold, *J. Eur. Ceram. Soc.* 5[1] (1989) 3-9.
20. E.Z. Solvas, D.D. Jayaseelan, H.T. Lin, P. Brown, and W.E. Lee, *J. Eur. Ceram. Soc.* 33 (2013) 1373-1386.